RSC Advances

PAPER

View Article Online
View Journal | View Issue

Cite this: *RSC Adv.*, 2020, **10**, 18572

Multiple-responsive supramolecular vesicle based on azobenzene–cyclodextrin host–guest interaction†

Jiao Wang, * Ting Wang, Xiaohui Liu, Yan Lu and Jingjing Geng

Multiple-responsive supramolecular vesicles have been successfully fabricated by the complexation between β-cyclodextrin (β-CD) and a pH/photo dual-responsive amphiphile 4-(4-(hexyloxy)phenylazo) benzoate sodium (HPB) with azobenzene and carboxylate groups. When mixing β-CD with HPB to reach a host/guest molar ratio of 1 : 1, the azobenzene group of HPB could be spontaneously included by β-CD molecules. Then, the formed inclusion complexes (HPB@β-CD) could self-assemble into vesicles, which was driven by the hydrophobic interaction of the alkyl chain of HPB and the hydrogen bonds between neighboring β-CDs. The reversible assembly/disassembly of the vesicles could be simply regulated under UV or visible light irradiation. The reversible phase transformation between vesicles and microbelts could also be realized by adjusting the pH values of the sample. Adding both competitive guest molecules (1-adamantane carboxylic acid sodium (ADA)) and α-amylase would result in the phase transformation from vesicles to micelles. Moreover, the vesicles would be destroyed when β-CD was continuously added until the ratio of host/guest reached 2 : 1. Such an interesting quintuple-responsive vesicle system reported here not only has potential applications in various fields such as controlled release or drug delivery, but also provides a reference for the design and construction of multiple responsive systems.

Received 6th March 2020
Accepted 8th May 2020

DOI: 10.1039/d0ra02123g

rsc.li/rsc-advances

1. Introduction

Amphiphiles can self-assemble into various well-organized structures in solution, such as micelles, vesicles, wires, lyotropic liquid crystals and gels.[1–8] These assemblies have been of great interest in recent years because of their widespread applications.[9–14] Among them, vesicles have been widely investigated due to their broad applications.[15–19] In addition, construction of stimuli-responsive vesicles endows them with special functions to develop biological systems, biosensors, and microreactors.[20–25] Therefore, research on stimuli-responsive vesicles has become a very fascinating topic.

Introducing sensitive groups (responsive to pH, redox reagents, salinity, enzymes and so on) into conventional amphiphilic molecules through covalent bonds can make the resulting ordered aggregates able to transform into desired structures, morphologies, and properties by external stimuli.[26–31] To make it easier, scientists turned their attention to supramolecular amphiphiles, which are built by the non-covalent interactions, such as hydrogen bonding, electrostatic interactions, host–guest inclusion and π–π stacking.[32–38] The amphiphilicity of the supramolecular amphiphiles can be adjusted by external stimuli because of their environmental sensitivity and reversibility. Therefore, the resulting ordered aggregates from supramolecular amphiphiles are able to respond to external stimuli.

Among the noncovalent interactions to construct supramolecular amphiphiles, the host–guest interaction has gained much more attention. The better complex-forming ability and low toxicity of cyclodextrins (CDs) make them to be a good choice for the host molecules to prepare responsive vesicles.[39–41] For example, Huang *et al.* prepared a system of spherical vesicles constructed by self-assembly of inclusion complexes formed by amphiphilic molecule (4-butyl-4′-(oxy-2,3-epoxypropyl) azobenzene, C_4AG) and β-CD in water.[42] The formed spherical vesicles were transformed into bacteria-like vesicles triggered by UV irradiation. Li *et al.* constructed a kind of UV/pH dual-responsive vesicles formed from supramolecular amphiphiles constructed by α-CD, azobenzene derivative (PPB) and dodecylamine.[43] Ravoo *et al.* reported the metal ion, light, and redox responsive vesicles through interaction of the modified β-CD and heterobifunctional azobenzene–ferrocene conjugates guest.[44] However, most of the stimuli-responsive vesicles reported focus on single stimulus or dual-stimuli such as pH/temperature, light/redox and UV/pH.[44–49] Only few multiple stimuli-responsive vesicle systems were reported and a broad exploration space was left. It is therefore desirable to develop more multiple

Department of Chemistry, Taiyuan Normal University, Jinzhong, 030619, China. E-mail: wangjiao@tynu.edu.cn

† Electronic supplementary information (ESI) available. See DOI: 10.1039/d0ra02123g

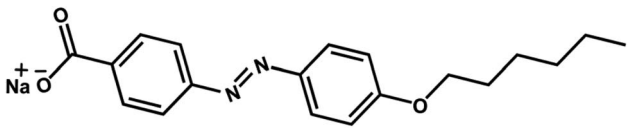

Fig. 1 The molecular structure of HPB.

stimuli-responsive vesicle systems because they can achieve more functions and can be adjusted by multiple parameters, which may present many interesting possibilities.

In this paper, quintuple-responsive vesicles were successfully constructed through the host–guest interaction between a synthesized anionic amphiphile with azobenzene and carboxylate group (HPB, as shown in Fig. 1) and β-CD. When β-CD was mixed with HPB in water to reach host/guest molar ratio of 1 : 1, vesicles were observed *via* the formation of supramolecular amphiphiles (HPB@β-CD). The alternant irradiation of UV and visible light would lead to the reversible assembly/disassembly of vesicles. Adjusting pH values of the solution could regulate the morphology of aggregates between vesicles and microbelts. Addition of both ADA and α-amylase would cause the vesicles to become micelles. Moreover, the formed vesicles could be destroyed by continued addition of β-CD in the same amount as the HPB@β-CD. Our results will be an important supplement to the growing body of literature regarding the multiple-responsive vesicle systems.

2. Experimental section

2.1 Materials

Benzocaine (99%), 1-bromohexane (98%), phenol (98%), α-amylase (98%) and β-CD (99%) were purchased from Aladdin Chemistry Company, Ltd. and used as received. The other reagents were analytical reagent (AR) grade and used directly without further purification.

2.2 Sample preparation of vesicle

The vesicle samples were prepared by mixing required β-CD and HPB in H_2O with the molar ratio of 1 : 1. The samples were homogenized ultrasonically for 30 min. Then they were incubated at 25 °C for 24 h before measurement. The concentration of HPB is expressed as the molar concentration of inclusion complexes. In order to ensure that *trans*-HPB excluded from the β-CD would not precipitate out of the solution after UV-light exposure due to its poor solubility, which would affect the reversibility of light response, the typical vesicle sample with the concentration of inclusion complexes at 0.1 mM was studied in this paper.

2.3 Synthesis of 4-(4-(hexyloxy)phenylazo)benzoate sodium

The final product, 4-(4-(hexyloxy)phenylazo)benzoate sodium (HPB), was synthesized according to the previously reported procedures.[50]

2.3.1 Synthesis of ethyl 4-((4-hydroxyphenyl)diazenyl) benzoate. Benzocaine (9.0 g) was dissolved in 80 mL hydrochloric acid aqueous solution (3 mM) below 5 °C. Then, $NaNO_2$ (4.54 g) dissolved in 31.4 mL H_2O was dropwise added by stirring below 5 °C for 30 min. Then, phenol (6.1 g) was added in batches into the resulted diazonium solution. This mixture was stirred below 5 °C for 1 h, and then stirred at room temperature for 6 h. The precipitation was observed by adding 100 mL saturated $NaCO_3$ aqueous solution. The brown precipitate was collected after filtration and then purified by recrystallization with ethanol three times and dried 48 h under vacuum. ^{1}H NMR ($CDCl_3$, 300 MHz, ppm): 8.20 (d, 2H), 7.92 (m, 4H), 6.97 (d, 2H), 4.42 (q, 2H), 1.43 (t, 3H).

2.3.2 Synthesis of ethyl 4-(4-(hexyloxy)phenylazo)benzoate. The ethyl 4-((4-hydroxyphenyl)diazenyl)benzoate (9.2 g), K_2CO_3 (9.4 g), potassium iodide (0.18 g) were mixed in acetone (120 mL) and refluxed for 10 min. Then 1-bromohexane (6.743 g) was added dropwise and kept refluxing for 24 h. After cooling down to room temperature, 200 mL H_2O was added. The resulted product was extracted with CH_2Cl_2 and then the organic layer was dried with $MgSO_4$. After filtration, the solvent was moved by vacuum rotary evaporation. The resulted precipitate was recrystallized from ethanol three times. ^{1}H NMR ($CDCl_3$, 300 MHz, ppm): 8.17 (m, 2H), 7.91 (m, 4H), 6.96 (m, 2H), 4.43 (q, 2H), 3.73 (m, 2H), 1.43 (m, 4H), 1.25 (m, 10H).

2.3.3 Synthesis of 4-(4-(hexyloxy)phenylazo)benzoate sodium. NaOH aqueous solution (25%, 30 mL) was added into ethyl 4-(4-(hexyloxy)-phenylazo)benzoate (5.63 g) in ethanol (150 mL), which was stirred at reflux for 5 h. Excess solvent was removed by vacuum rotary evaporation. The yellow precipitate was recrystallized three times from dilute NaOH aqueous solution. ^{1}H NMR: (DMSO-d_6, 300 MHz, ppm): 8.12 (d, 2H), 7.92 (m, 4H), 7.15 (d, 2H), 4.09 (t, 2H), 1.75 (m, 2H), 1.43 (m, 2H), 1.32 (m, 4H), 0.89 (t, 3H). HR-MS (ESI): *m*/*z* calc. for $C_{19}H_{21}N_2O_3$: 325.1558; found, 325.1425. Elemental analysis: calc. (%) for $C_{19}H_{21}N_2O_3Na$: C 65.51, H 6.08, N 8.04; found: 65.59, H 6.19, N 8.02.

2.4 Characterization

2.4.1 Dynamic light scattering (DLS) measurement. DLS measurements were performed by a Brookhaven BI-200SM Instrument equipped with an argon laser (k = 532 nm) at 25 °C. The results obtained were analyzed by the CONTIN method.

2.4.2 Fourier transformed infrared (FTIR) spectroscopy measurement. An appropriate amount of solid sample and KBr were compressed into a transparent disk, which was measured on an Alpha-T spectrometer (Bruker) from 400 to 4000 cm^{-1}. For the vesicle sample, the solution was freeze-dried for 48 h into a solid.

2.4.3 2D ^{1}H–^{1}H ROESY measurement. The samples were determined on a Bruker Advance 500 spectrometer at 25 °C. The samples were prepared by mixing HPB, β-CD and D_2O at desired proportions. These mixtures were homogenized ultrasonically for 30 min and then kept at 25 °C for 24 h before measurement.

2.4.4 Atomic force microscopy (AFM) measurement. A drop of sample was placed on a mica surface and the excess sample was wicked away by a filter paper. This substrate was air-dried

and observed using a Nanoscope IIIA from Digital Instruments under ambient conditions operating in tapping mode.

2.4.5 Transmission electron microscopy (TEM) measurement. The morphology of aggregates was observed by TEM (JEM-100CX II, Japan). About 4 μL of sample solution was placed onto a copper grid covered with formvar support film. After 15 s, excess solution was removed carefully using a strip of filter paper and then stained by 2.0 wt% uranyl acetate aqueous solution.

2.4.6 UV-vis spectroscopy measurement. The UV-vis spectra of sample were performed on a HP-8453 spectrometer. For light irradiation, a CHF-XM35-500W ultrahigh pressure short arc xenon lamp with optical filters (365 nm) was used.

2.4.7 Scanning electron microscopy (SEM) measurement. A drop of sample was put onto a silicon wafer. The excess sample was removed by filter paper. The sample was then freeze-dried for 12 h. SEM images were measured by a Hitachi S-4800 SEM system.

2.4.8 X-ray diffraction (XRD) measurement. XRD measurement of the dried microbelts was performed between 1 and 20° on a Rigaku D/Max 2200-PC diffractometer with a Cu-Kα radiation (0.15406 nm).

3. Results and discussion

3.1 Characterization for HPB/β-CD inclusions

Both the azobenzene and alkyl chain in HPB could be included by β-CD. The chemical shift change of H-5 of β-CD was used to check the maximum host/guest inclusion ratio by the Job's plot (Fig. S1†). Its maximum at $r = [\beta\text{-CD}]/([\beta\text{-CD}] + [\text{HPB}]) = 0.65$ indicates 1 : 2 stoichiometry, *i.e.* the HPB molecule could be included by two β-CDs at most.

To verify the host–guest interaction of HPB and β-CD in 1 : 1 (HPB : β-CD) system, 2D rotating-frame overhauser enhancement spectroscopy (ROESY) measurement was applied. Two cross-peak signals (marked with blue squares) between protons of the azobenzene moiety of HPB and β-CD can be observed in Fig. 2. However, no signal indicating interactions of alkyl chain and β-CD is observed, which excludes the inclusion there.[51] This result is attributed to the bigger association constant between azobenzene (about 1.25–2.66 × 10^3 M^{-1}) and β-CD comparing with the alkyl chain similar to HPB (about 3.70–8.60 × 10^2 M^{-1}) according to the reported literatures.[37,52–55] Therefore, the ROESY spectrum clearly indicates that only azobenzene group

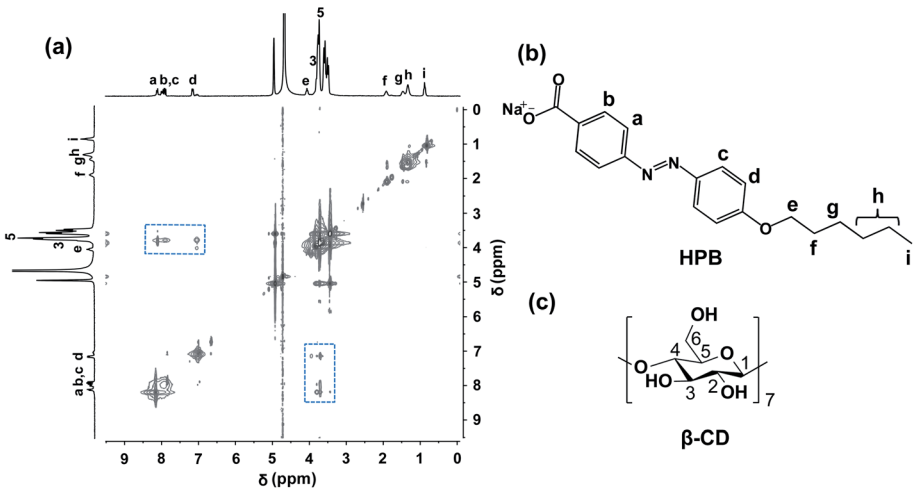

Fig. 2 ^1H–^1H 2D ROESY NMR spectrum for 5 mM HPB@β-CD in D_2O at 25 °C (a) and chemical structures of HPB (b) and β-CD (c).

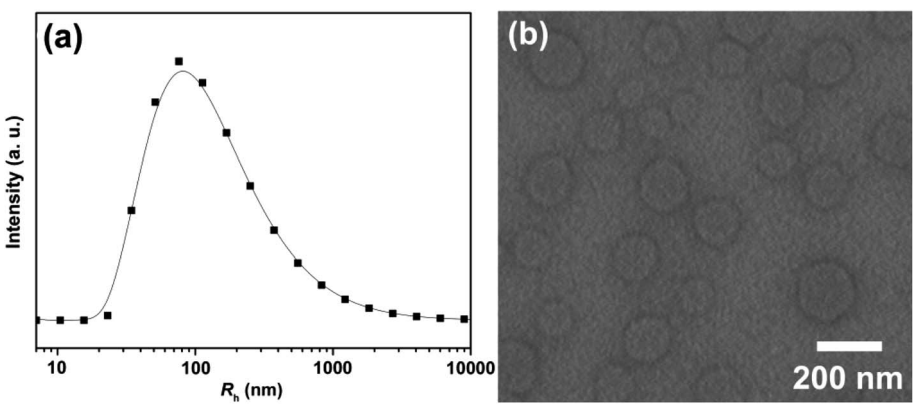

Fig. 3 Hydrodynamic radius (R_h) distribution determined by DLS (a) and TEM (b) for 0.1 mM HPB@β-CD aqueous solution at 25 °C.

was included by β-CD, resulting in the formation of supramolecular complexes (recorded as HPB@β-CD).[56,57]

3.2 Vesicles formed by HPB@β-CD

The critical aggregation concentration (CAC) of HPB@β-CD was determined by DLS measurement (Fig. S2†). No signals were detected when the concentration of HPB@β-CD was less than 0.05 mM, indicating no ordered aggregates formation. When the concentration of HPB@β-CD was greater than 0.05 mM, aggregates with average hydrodynamic radius value about 80–90 nm could be detected, which indicates that the CAC of HPB@β-CD is 0.05 mM. The morphology and size of aggregate structures from HPB@β-CD aqueous solution were investigated by DLS, TEM and AFM, respectively. From the Fig. 3a, we can see that the average hydrodynamic radius (R_h) value of aggregates is mapped as around 80 nm. To give more direct evidence, the negatively staining TEM was applied. Large amounts of vesicles with diameters from about 60 to 180 nm can be observed in Fig. 3b.

To confirm the molecular arrangement of HPB@β-CD in the vesicle wall, the dehydrated vesicles were tested by AFM. As shown in Fig. 4a, the spherical vesicles were detected, which agree well with those obtained from TEM result. The larger diameter/height ratio (about 20) of the two collapsed vesicles can be read from the section analysis profile (Fig. 4b), which also verifies that the structure is vesicular. The heights of the two collapsed vesicles are 7.12 and 6.93 nm, which are the thickness of two closely stacked membranes of the vesicles. One half of the thickness can be considered as the membrane thickness of the vesicle wall. The average membrane thickness of the vesicle is therefore calculated to be about 3.5 nm, which is shorter than twice the length of HPB@β-CD (4.26 nm) from the density functional theory (DFT) calculation carried out by the Gaussian 09 package with the B3LYP functional and the 6-31G(d,p) basis set, as shown in Fig. 4c. This result indicates an interdigitated antiparallel arrangement for HPB@β-CD inclusion complexes in the vesicle.

A large of number hydroxyl groups of β-CDs can form hydrogen bonds which can promote the inclusion complexes aggregation. To examine this, the FTIR spectra of the vesicles, β-CD and HPB were analyzed, with the results shown in Fig. S3.† The characteristic peaks of –OH group of pure β-CD (3405 cm^{-1}) and carboxylate ($–COO^-$) group in pure HPB (1546 cm^{-1} and 1418 cm^{-1}) can be found in the spectra of pure β-CD and HPB, respectively. However, in vesicle, such –OH absorption peak shifts to a lower frequency at 3392 cm^{-1}. As is well known, the association of –OH groups makes the absorption peak shift to

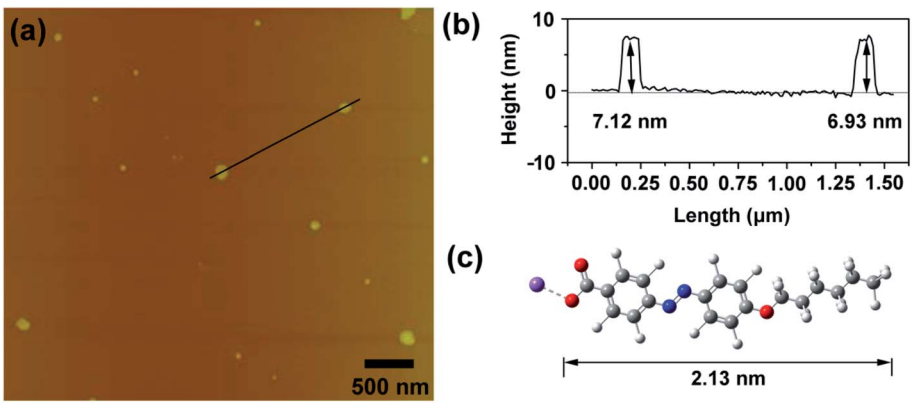

Fig. 4 (a) AFM image of dehydrated vesicles from 0.1 mM HPB@β-CD sample. (b) Height profile plot of the two selected vesicles. (c) Molecular structure model of HPB.

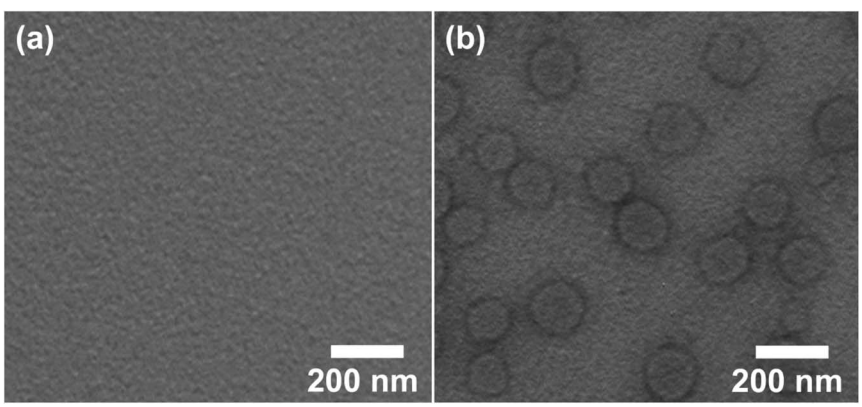

Fig. 5 TEM images of 0.1 mM HPB@β-CD aqueous solution after UV irradiation (a) and then treated with visible light (b).

a lower frequency. Thus, this change of absorption peak position reflects the intermolecular hydrogen bonding between β-CDs.[58,59] In addition, there is no change in position of $-COO^-$ stretching absorption peak of HPB and vesicle, indicating no hydrogen bonding between HPB and β-CD.

3.3 Photo-responsiveness of vesicles

Azobenzene group of HPB can undergo *trans*-to-*cis* isomerization upon UV light irradiation and the transformed *cis*-forms can return back to their *trans*-forms when the irradiated sample is then treated with visible light, which therefore may result in the reversible assembly/disassembly of the vesicles. DLS was applied first to explore the variation of the aggregate size of the 0.1 mM HPB@β-CD aqueous solution after UV irradiation. After UV lamp treatment, no signals were detected from DLS measurement, indicating no ordered aggregates in the solution. Of great interest, R_h at about 77 nm can be observed again followed by visible-light exposure (Fig. S4†). This result indicates that the vesicles were formed again.

To verify the above proposal, TEM was used with the results shown in Fig. 5. From the Fig. 5a, any detectable regular aggregates were observed from the HPB@β-CD aqueous solution after UV irradiation. More importantly, vesicles could be reformed followed by visible light irradiation (Fig. 5b), which is in agreement with the DLS result described above. It can be concluded that the vesicles experiences reversible photo-responsiveness.

Such a photo induced phase transformation can be tracked using UV-vis absorption spectra. As shown in Fig. 6a for absorbance spectra of HPB@β-CD aqueous solution, the absorption band at 356 nm is ascribed to π–π* transition of *trans*-HPB before UV irradiation.[42,60] A remarkable decrease in intensity and an obvious blue shift of this absorption peak can be clearly observed after UV light irradiation. Moreover, a slight absorbance increase of a band at 428 nm is observed. This change in absorption indicates the *trans*-to-*cis* photoisomerization of HPB.[42,60] After UV light irradiation for 5 min, such the *trans*-to-*cis* photoisomerization reached equilibrium and the maximum isomerization efficiency reached to 65.7%, calculated from the intensity of π–π* absorption band before and after UV irradiation.[61–63] The *cis*-HPB could return back to their *trans*-forms again after the irradiated sample treated with visible light irradiation. As shown in Fig. 6b, such photoisomerization behavior could repeat many times.

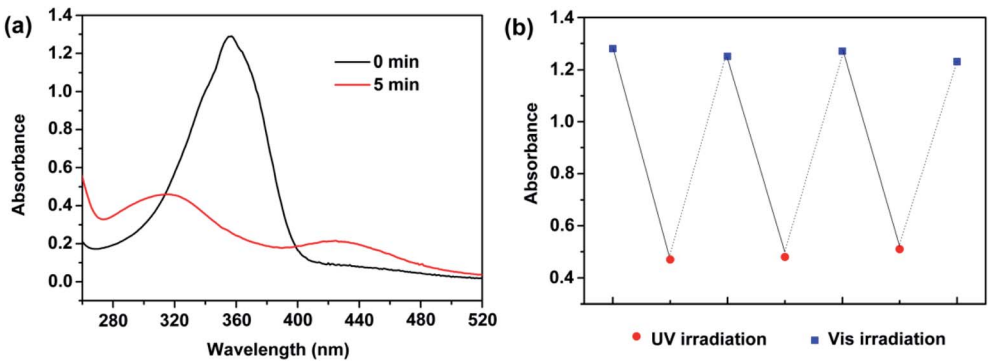

Fig. 6 (a) UV-vis absorption spectra of 0.1 mM HPB@β-CD aqueous solution before and after UV-light irradiation for 5 min; (b) absorbance at 316 (red) and 356 nm (blue) by alternate irradiation by UV and visible light, respectively.

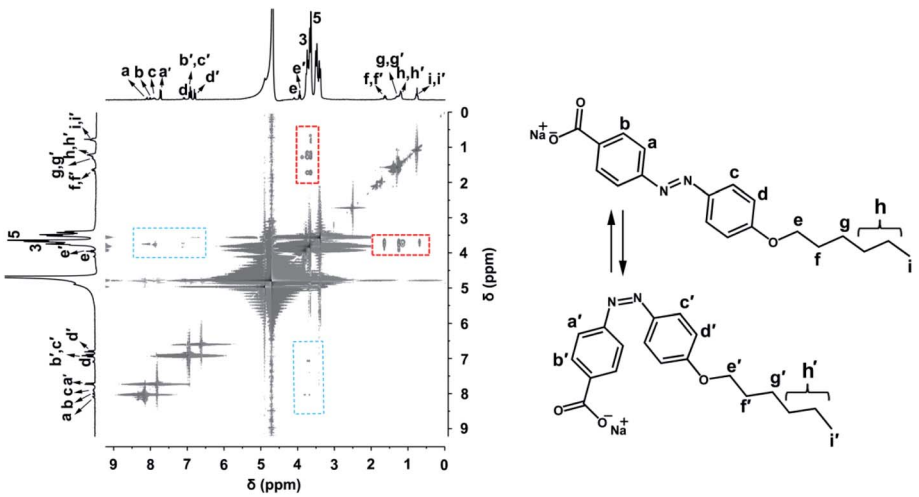

Fig. 7 $^1H-^1H$ 2D ROESY NMR spectrum for 5 mM HPB@β-CD in D_2O after UV irradiation.

To investigate the inclusion behavior of HPB and β-CD after UV exposure, 2D ^{1}H–^{1}H ROESY spectra was applied. As shown in Fig. 7, *trans*- and *cis*-HPB coexisted in the solution and the percentage of *cis*-forms reached to 64.9% (calculated from the integral intensity values of aromatic protons of both *trans*- and *cis*-azobenzene), in agreement with the result from UV-vis spectra. In addition, apart from the interactions between the azobenzene of *trans*-HPB and β-CDs (marked with blue squares), the cross-peak signals between protons of the alkyl chain and β-CDs (marked with red squares) can also be seen. These results indicate that the azobenzene of *trans*-HPB was still included by β-CD, but the azobenzene of *cis*-HPB was excluded from the cavity of β-CD because of its bulky volume. Then, the alkyl chain of both *trans*- and *cis*-HPB could be included by the dropped β-CD. Therefore, it can be concluded that four kinds of molecules (HPB@β-CD, HPB@2β-CD, *cis*-HPB@β-CD and *cis*-HPB, as shown in Fig. S5†) may coexist in the solution after UV exposure.

Based on the above discussions, the reason for such a photo-responsiveness behavior is based on the HPB@β-CD formation and destruction. Driven by van der Waals and hydrophobic interactions, azobenzene of *trans*-HPB was included by β-CD, causing the formation of supramolecular complexes HPB@β-CD. Then, the formed HPB@β-CD could self-assemble into vesicles, which was driven by hydrophobic interaction of alkyl chain of HPB and the hydrogen bonds between neighboring β-CDs. When the vesicle system was exposed to UV light, most of the *trans*-azobenzene groups were converted into *cis*-forms with bigger volume to be released from the cavity of β-CDs, leading to the destruction of HPB@β-CD. The concentration of the retained HPB@β-CD in the solution was too low to form vesicles and the other three kinds of molecules (HPB@2β-CD, *cis*-HPB@β-CD and *cis*-HPB) could also not form any aggregates. All of these resulted in the disassembly of the vesicle. Under visible-light irradiation of the UV irradiated sample, *cis*-HPB was converted back into *trans*-forms and was included by β-CD, resulting in the regeneration of vesicle again.

3.4 pH-Responsiveness of vesicle

In view of the reversible pH-responsiveness of carboxylate head group of HPB, we considered that the morphology of vesicles can also be reversibly controlled by adjusting pH values. As it has been found, HPB@β-CD could self-assemble into vesicles. When the pH value was decreased to 4.5, significant changes of morphology occurred. As shown in Fig. 8a, the vesicles disassembled and a lot of long (several tens of microns) belt-like aggregates appeared. When the pH value was raised to 9.8 (the sample was then heated to 80 °C to obtain transparent solution and incubated at 25 °C for 24 h), the vesicles could be surprisingly reformed again (Fig. 8b). This phase transformation from vesicle to belt-like aggregates may be attributed to that as the pH values of the solution decreased, the carboxylate head group of HPB molecules was protonated into carboxylic acid group, which decreased the repulsion between HPB@β-CD complexes to promote formation of aggregates with larger critical packing parameter.

To explore the molecular arrangement of protonated HPB@β-CD in the microbelts, XRD measurement was applied. As shown in Fig. S6,† three diffraction peaks ($2\theta = 2.43°$, $4.88°$ and $7.23°$) with d spacings of 3.63, 1.82, and 1.22 nm (with a ratio of 1 : 1/2 : 1/3) can be observed, indicating a typical lamellar structure.[64] The d spacing of 3.63 nm calculated from the first order diffraction peak is shorter than twice the length of HPB@β-CD (4.26 nm). Thus, these results imply that the lamellar microbelts from the self-assembly of protonated HPB@β-CD are composed of bilayer structures with an interdigitated antiparallel arrangement.

3.5 ADA, α-amylase and β-CD responsiveness of vesicle

As is well-known, various types of guest molecules can be included by β-CD to form inclusion complexes but with different association constants.[40,41] So, responsive vesicle system can be constructed by adding competitive guest molecules. Herein, ADA was chosen due to its high association constant with β-CD. When the same amount of ADA molecules as HPB@β-CD was added to the solution, the vesicles were transformed into micelles. As observed in Fig. S7a,† the R_h of micelles was around 8 nm. These spherical micelles were also observed by TEM observation (Fig. S7b†), which was almost consistent with those observed from the DLS. This result may be attributed to that β-CD released the azobenzene of HBP and

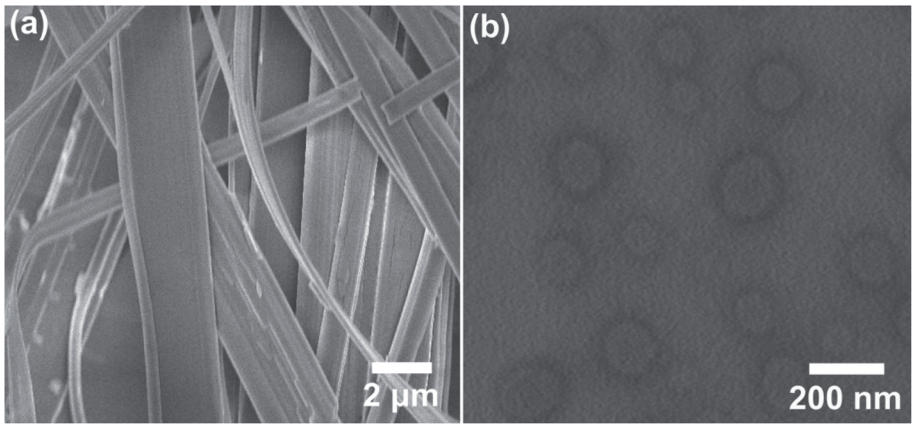

Fig. 8 SEM (a) and TEM (b) images of 0.1 mM HPB@β-CD self-assemblies at different pH values: 4.5 (a) and 9.8 (b).

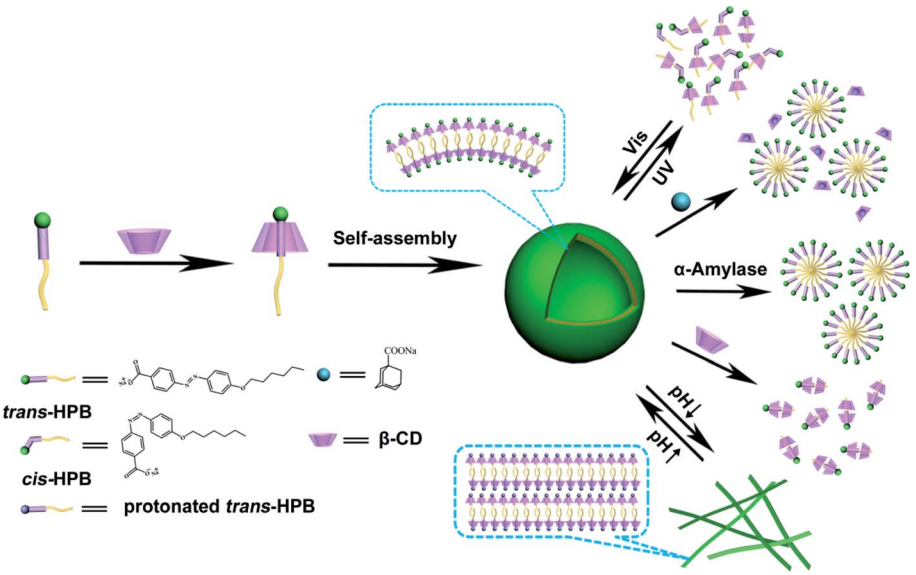

Fig. 9 The schematic representations of multiple-responsive vesicles.

then included the adamantane group due to the bigger association constant between adamantane group and β-CD comparing with the azobenzene.[40,41] Then, the HPB itself self-assembled into micelles.

Enzyme-responsive systems, referring to systems controlled by enzymes, are important in smart assemblies. α-Amylase can hydrolyze β-CD into sugars.[65] Therefore, α-amylase was selected to prepare the enzyme-responsive vesicle system. α-Amylase with a gravity of 0.5 g/5 mL was added into the vesicle system. Then enzymatic reactions were carried out at 37 °C for 48 h. The TEM result (Fig. S8†) indicates that after adding α-amylase, β-CD was hydrolyzed from HPB@β-CD, which consequently shattered the vesicles into micelles due to the transformation of HPB@β-CD complex into HPB. Then, pure HPB self-assembled into micelles.

It is well-established that the alkyl chain of HPB@β-CD is also able to be included by β-CD. Here we used the tendency of β-CDs to form complexes with alkyl chain of HPB@β-CD to adjust the hydrophobicity of building blocks to construct β-CD responsive vesicle system. As expected, when we added β-CD into HPB@β-CD vesicle system to reach host/guest (β-CD/HPB) molar ratio of 2 : 1, no ordered aggregates could be observed from both DLS and TEM measurements. This result indicates the disassembly of the vesicles upon adding superabundant β-CD, which is probably due to the increase of the hydrophobicity of alkyl chain of HPB@β-CD after included by β-CD. Meanwhile, the formed HPB@2β-CD concentration is too low to form aggregates driven by hydrogen bond between β-CDs. Based on all the results described above, the multiple-responsiveness mechanism can be assumed, as shown in Fig. 9.

4. Conclusions

In conclusion, a newly synthesized anionic amphiphile (HPB) containing carboxylate and azobenzene groups could form inclusion complexes (HPB@β-CD) by adding β-CD to reach *R* value of 1 : 1. The resulted HPB@β-CD could form vesicles, which was driven by the hydrophobic interaction of alkyl chain of HPB and hydrogen bonds between β-CDs. More noticeably, the obtained vesicles were responsive to UV light, pH, β-CD, α-amylase and ADA, which benefited from the photo/pH responsiveness of HPB, competitive host–guest complexing, hydrolyzation of β-CD by amylase and the host–guest interaction between alkyl chain of HPB@β-CD and β-CD. Considering the good responsiveness, economical preparation and the advantage of responding to various external stimuli, such quintuple-responsive vesicle system could not only find broad applications, but also easily adapts to multiple-responsive assembly of other materials.

Conflicts of interest

There are no conflicts to declare.

Acknowledgements

We are thankful for the financial support from the Scientific and Technological Innovation Programs of Higher Education Institutions in Shanxi (2019L0795).

References

1 S. Svenson, *Curr. Opin. Colloid Interface Sci.*, 2004, **9**, 201–212.
2 Q. T. Li, X. D. Wang, X. Yue and X. Chen, *Soft Matter*, 2013, **9**, 9667–9674.
3 T. G. Barclay, K. Constantopoulos and J. Matisons, *Chem. Rev.*, 2014, **114**, 10217–10291.

4 T. F. A. De Greef, M. M. J. Smulders, M. Wolffs, A. P. H. J. Schenning, R. P. Sijbesma and E. W. Meijer, *Chem. Rev.*, 2009, **109**, 5687–5754.
5 Y. Wang, Z. C. Pei, W. W. Feng and Y. X. Pei, *J. Mater. Chem. B*, 2019, **48**, 7656–7675.
6 X. J. Zhao, X. L. Yu, Y. Lee and H. G. Liu, *Langmuir*, 2016, **32**, 11819–11826.
7 Z. L. Chu, C. A. Dreiss and Y. J. Feng, *Chem. Soc. Rev.*, 2013, **17**, 7174–7203.
8 S. Bruno, G. Chiabotto, E. Favaro, M. C. Deregibus and G. Camussi, *Am. J. Physiol.: Cell Physiol.*, 2019, **317**, 303–313.
9 X. P. Gao, B. Dong, F. Lu, T. Zhou, W. F. Tian and L. Q. Zheng, *Chem. Commun.*, 2014, **50**, 8783–8786.
10 W. T. Wang, Y. C. Han, M. Z. Tian, Y. X. Fan, Y. Q. Tang, M. Y. Gao and Y. L. Wang, *ACS Appl. Mater. Interfaces*, 2013, **5**, 5709–5716.
11 Y. Hyunwoo, B. Y. Lu and X. H. Zhao, *Chem. Soc. Rev.*, 2019, **48**, 1642–1667.
12 X. F. Ji, Y. Yao, J. Y. Li, X. Z. Yan and F. H. Huang, *J. Am. Chem. Soc.*, 2012, **135**, 74–77.
13 R. Mezzenga, J. M. Seddon, C. J. Drummond, B. J. Boyd, G. E. Schröder-Turk and L. Sagalowicz, *Adv. Mater.*, 2019, **31**, 1900818–1900821.
14 S. Biswas, P. Kumari, P. M. Lakhani and B. Ghosh, *Eur. J. Pharm. Sci.*, 2016, **83**, 184–202.
15 X. Zhang, S. Rehm, M. M. Safont-Sempere and F. Würthner, *Nat. Chem.*, 2009, **1**, 623–629.
16 T. Huang, H. Li, L. Huang, S. Li, K. Li and Y. Zhou, *Langmuir*, 2016, **32**, 991–996.
17 K. Valdés, M. J. Morilla, E. Romero and J. Chávez, *Colloids Surf., B*, 2014, **117**, 1–6.
18 S. Dergunov, A. Khabiyev, S. Shmakov, M. Kim, N. Ehterami, M. Weiss, V. Birman and E. Pinkhassik, *ACS Nano*, 2016, **10**, 11397–11406.
19 M. B. Dipl.-Chem, S. Burghardt, C. Bottcher, T. Bayerl, S. Bayerl and A. Hirsch, *Angew. Chem., Int. Ed.*, 2000, **39**, 1845–1848.
20 Q. P. Duan, Y. Cao, Y. Li, X. Y. Hu, T. X. Xiao, C. Lin and L. Y. Wang, *J. Am. Chem. Soc.*, 2013, **135**, 10542–10549.
21 S. Ganta, H. Devalapally, A. Shahiwala and M. Amiji, *J. Controlled Release*, 2008, **126**, 187–204.
22 X. Yang, J. J. Grailer, I. J. Rowland, A. Javadi, S. A. Hurley, V. Z. Matson and S. Gong, *ACS Nano*, 2010, **4**, 6805–6817.
23 H. Y. Lee, K. R. Tiwari and S. R. Raghavan, *Soft Matter*, 2011, **7**, 3273–3276.
24 J. L. Shen, X. Xin, T. Liu, S. B. Wang, Y. J. Yang, X. Y. Luan, G. Y. Xu and S. L. Yuan, *Langmuir*, 2016, **37**, 9548–9556.
25 U. Kauscher, M. N. Holmed, M. Björnmalm and M. M. Stevensa, *Adv. Drug Delivery Rev.*, 2019, **138**, 259–275.
26 Z. Jiang, J. Liu, K. Sun, J. F. Dong, X. F. Li, S. Z. Mao, Y. R. Du and M. L. Liu, *Colloid Polym. Sci.*, 2014, **292**, 739–747.
27 X. N. Jing, Z. Zhi, L. M. Jin, F. Wang, Y. S. Wu, D. Q. Wang, K. Yan, Y. P. Shao and L. J. Meng, *Nanoscale*, 2019, **11**, 9457–9467.
28 S. K. M. Nalluri and B. J. Ravoo, *Angew. Chem., Int. Ed.*, 2010, **49**, 5371–5374.
29 L. L. Fu, J. Q. Jiang, B. X. Lu, Y. L. Xu and J. Zhai, *ChemNanoMat*, 2019, **5**, 1182–1187.
30 D. S. Guo, K. Wang, Y. X. Wang and Y. Liu, *J. Am. Chem. Soc.*, 2012, **134**, 10244–10250.
31 J. H. Zhu, Y. M. Niu, Y. Li, Y. X. Gong, H. H. Shi, Q. Huo, Y. Liu and Q. W. Xu, *J. Mater. Chem. B*, 2017, **5**, 1339–1352.
32 H. L. Zhao, X. Song, H. Aslan, B. Liu, J. G. Wang, L. Wang and M. D. Dong, *Phys. Chem. Chem. Phys.*, 2016, **18**, 14168–14171.
33 Y. T. Kang, K. Liu and X. Zhang, *Langmuir*, 2014, **30**, 5989–6001.
34 X. Zhang and C. Wang, *Chem. Soc. Rev.*, 2011, **40**, 94–101.
35 Y. Y. Ai, Y. G. Li, H. L. Fu, A. K. Chan and V. W. Yam, *Chem.–Eur. J.*, 2019, **25**, 5251–5258.
36 K. Liu, Y. T. Kang, Z. Q. Wang and X. Zhang, *Adv. Mater.*, 2013, **25**, 5530–5548.
37 F. Xie, G. H. Ouyang, L. Qin and M. H. Liu, *Chem.–Eur. J.*, 2016, **22**, 18208–18214.
38 Y. Yan, J. B. Huang and B. Z. Tang, *Chem. Commun.*, 2016, **52**, 11870–11884.
39 Q. H. Li, A. X. Li, W. Sun and T. Zhang, *J. Chin. Chem. Soc.*, 2016, **63**, 930–934.
40 A. J. M. Valente and O. Söderman, *Adv. Colloid Interface Sci.*, 2014, **205**, 156–176.
41 L. X. Jiang, Y. Yan and J. B. Huang, *Adv. Colloid Interface Sci.*, 2011, **169**, 13–25.
42 Q. Zhao, Y. Wang, Y. Yan and J. B. Huang, *ACS Nano*, 2014, **8**, 11341–11349.
43 S. Y. Li, A. Y. Hao, J. Shen, N. Z. Shang and C. Wang, *Soft Matter*, 2018, **14**, 2112–2117.
44 A. Samanta and B. J. Ravoo, *Chem.–Eur. J.*, 2014, **20**, 4966–4973.
45 K. Wang, D. S. Guo, X. Wang and Y. Liu, *ACS Nano*, 2011, **5**, 2880–2894.
46 P. P. Sun, A. L. Wu, N. Sun, X. X. Qiao, L. J. Shi and L. Q. Zheng, *Langmuir*, 2018, **34**, 791–2799.
47 A. Samanta and B. J. Ravoo, *Chem.–Eur. J.*, 2014, **20**, 4966–4973.
48 P. Y. Xing, T. Sun and A. Y. Hao, *RSC Adv.*, 2013, **3**, 24776–24793.
49 T. F. Yan, F. Li, S. W. Qi, J. Tian, R. Z. Tian, J. X. Hou, Q. Luo, Z. Y. Dong, J. Y. Xu and J. Q. Liu, *Chem. Commun.*, 2020, **56**, 149–152.
50 R. M. Yang, S. H. Peng and T. C. Hughes, *Soft Matter*, 2014, **10**, 2188–2196.
51 Z. Zhai, L. Lei and J. Song, *Soft Matter*, 2016, **12**, 2715–2720.
52 J. Moratz, L. Stricker, S. Engel and B. J. Ravoo, *Macromol. Rapid Commun.*, 2017, **39**, 1700256–1700261.
53 J. B. Li, X. F. Li, H. Liu, T. Ren, L. Huang, Z. W. Deng, Y. J. Yang and S. A. Zhong, *Polym. Degrad. Stab.*, 2019, **168**, 108956–108964.
54 S. Lima, B. J. Goodfellow and J. J. C. Teixeira-Dias, *J. Phys. Chem. A*, 2004, **108**, 10044–10049.
55 J. Li, C. G. Ji, X. Q. Yu, M. Z. Yin and D. Kuckling, *Macromol. Rapid Commun.*, 2019, **40**, 1900189–1900194.
56 L. Yue, S. Wang, D. Zhou, H. Zhang, B. Li and L. X. Wu, *Nat. Commun.*, 2016, **7**, 10742–10752.

57 L. Yue, H. Ai, Y. Yang, W. Lu and L. X. Wu, *Chem. Commun.*, 2013, **49**, 9770–9772.
58 L. X. Jiang, Y. Yan and J. B. Huang, *Soft Matter*, 2011, **7**, 10417–10423.
59 J. L. Shen, J. Y. Pang, T. Kalwarczyk, R. Holyst, X. Xin, G. Y. Xu, Y. X. Luan and Y. J. Yang, *J. Mater. Chem. C*, 2015, **3**, 8104–8113.
60 A. L. Wu, F. Lu, P. P. Sun, X. P. Gao, L. J. Shi and L. Q. Zheng, *Langmuir*, 2016, **32**, 8163–8170.
61 L. Stricker, E. C. Fritz, M. Peterlechner, N. L. Doltsinis and B. J. Ravoo, *J. Am. Chem. Soc.*, 2016, **138**, 4547–4554.
62 C. E. Weston, R. D. Richardson, P. R. Haycock, A. J. P. White and M. J. Fuchter, *J. Am. Chem. Soc.*, 2014, **136**, 11878–11881.
63 S. M. Gan, A. R. Yuvaraj, M. R. Lutfor and M. Y. Mashitah, *RSC Adv.*, 2015, **5**, 6279–6285.
64 Y. J. Wang, P. Y. Xing, S. Y. Li, M. F. Ma, M. M. Yang, Y. M. Zhang, B. Wang and A. Y. Hao, *Langmuir*, 2016, **32**, 10705–10711.
65 Y. T. Kang, Z. G. Cai, X. Y. Tang, K. Liu, G. T. Wang and X. Zhang, *ACS Appl. Mater. Interfaces*, 2016, **8**, 4927–4933.